

# Regulation and Function of the CD3 $\gamma$ DxxxLL Motif: A Binding Site for Adaptor Protein-1 and Adaptor Protein-2 in Vitro

Jes Dietrich, Jesper Kastrup, Bodil L. Nielsen, Niels Ødum, and Carsten Geisler

Institute of Medical Microbiology and Immunology, University of Copenhagen, The Panum Institute, DK-2200 Copenhagen, Denmark

**Abstract.** Several receptors are downregulated by internalization after ligand binding. Regulation of T cell receptor (TCR) expression is an important step in T cell activation, desensitization, and tolerance induction. One way T cells regulate TCR expression is by phosphorylation/dephosphorylation of the TCR subunit clusters of differentiation (CD)3 $\gamma$ . Thus, phosphorylation of CD3 $\gamma$  serine 126 (S126) causes a downregulation of the TCR. In this study, we have analyzed the CD3 $\gamma$  internalization motif in three different systems in parallel: in the context of the complete multimeric TCR; in monomeric CD4/CD3 $\gamma$  chimeras; and in vitro by binding CD3 $\gamma$  peptides to clathrin-coated vesicle adaptor proteins (APs). We find that the CD3 $\gamma$  D<sup>127</sup>xxxLL<sup>131/132</sup> sequence represents one united motif for binding of both AP-1 and AP-2, and that this motif functions as an active sorting motif in monomeric CD4/

CD3 $\gamma$  molecules independently of S126. An acidic amino acid is required at position 127 and a leucine (L) is required at position 131, whereas the requirements for position 132 are more relaxed. The spacing between aspartic acid 127 (D127) and L131 is crucial for the function of the motif in vivo and for AP binding in vitro. Furthermore, we provide evidence indicating that phosphorylation of CD3 $\gamma$  S126 in the context of the complete TCR induces a conformational change that exposes the DxxxLL sequence for AP binding. Exposure of the DxxxLL motif causes an increase in the TCR internalization rate and we demonstrate that this leads to an impairment of TCR signaling. On the basis of the present results, we propose the existence of at least three different types of L-based receptor sorting motifs.

**T**HE establishment and maintenance of self-tolerance is based on multiple events in the thymus and periphery resulting in either deletion of self-reactive T cells or induction of nonresponsiveness (for review see reference 22). Transgenic models of peripheral nonresponsiveness have demonstrated that T cell tolerance can be maintained by downregulation of the T cell receptor (TCR)<sup>1</sup> and/or of clusters of differentiation (CD)4 or CD8 (10, 37, 40, 47). In addition, downregulation of the TCR, CD4, and CD8 has also been observed in the process of tolerance induction to Mls-1<sup>a</sup> in nontransgenic mice (18). Thus, it has been proposed that peripheral tolerance induction is a multistep process characterized by the phenotypic appearance of the tolerant T cells. This ranges from a relative

mild form of tolerance without any phenotypic changes to the most stringent level of anergy with complete downregulation of the TCR (1). In addition to the process of tolerance induction, TCR downregulation has been observed during T cell activation and it has been proposed that TCR downregulation might be crucial for T cell activation in allowing serial triggering of many TCRs by few peptide-major histocompatibility complexes (49, 50). The mechanisms involved in downregulation of the TCR and coreceptors at the T cell surface are still not fully known.

Several receptors associated with tyrosine kinase activity are downregulated by internalization following ligand binding. Internalization of these receptors takes place via clathrin-coated vesicles and requires a tyrosine-based (Y-based) sorting motif in the cytoplasmic tail of the receptors (for reviews see references 27, 48, 53). A direct interaction between clathrin-coated vesicle adaptor proteins (APs) and Y-based sorting motifs has been shown for some of these receptors (2, 13, 30–32, 44, 45). The APs are a major component of clathrin-coated pits and vesicles. At least two different forms of AP complexes exist: AP-1, composed of the ~100-kD  $\gamma$ - and  $\beta$ 1-adaptin, and the smaller ~47-kD  $\mu$ 1 and ~20-kD  $\sigma$ 1 subunits, is found in association with clathrin at the TGN; and AP-2, composed of the ~100-kD  $\alpha$ - and  $\beta$ 2-adaptin and the smaller ~50-kD

Please address all correspondence to Carsten Geisler, Institute of Medical Microbiology and Immunology, University of Copenhagen, The Panum Institute, Building 18.3, Blegdamsvej 3C, DK-2200 Copenhagen, Denmark. Tel.: (45) 3532-7880. Fax: (45) 3532-7881. e-mail: cgetr@biobase.dk

1. *Abbreviations used in this paper:* AP, adaptor protein; CD, clusters of differentiation; EGFR, epidermal growth factor receptor; Ii, invariant chain; JGN, Jurkat gamma negative; MFI, mean fluorescence intensity; PDB, phorbol 12,13-dibutyrate; PE, phycoerythrin; PKC, protein kinase C; TCR, T cell receptor.

$\mu 2$  and  $\sim 17$ -kD  $\sigma 2$  subunits, is found in association with clathrin at the plasma membrane (for review see references 33, 36).

In addition to Y-based motifs, other motifs involved in receptor internalization and sorting have been described. Leucine-based (L-based) sorting motifs, usually composed of two successive leucines, have been identified both in receptors internalized from the plasma membrane (4, 6, 9, 23, 43) and in receptors sorted from the TGN to endosomes/lysosomes (19, 23, 39). Whether AP complexes bind to L-based sorting motifs remains to be determined.

Internalization of some plasma membrane receptors with L-based sorting motifs is dependent on phosphorylation of a serine located five residues amino terminal to the motif (6, 42, 43). This raises the possibility that some L-based internalization motifs may be inaccessible in the nonphosphorylated state and become accessible/activated after receptor phosphorylation, as previously suggested (7). The TCR and CD4 represent receptors with L-based sorting motifs that are internalized from the plasma membrane via clathrin-coated pits after protein kinase C (PKC)-mediated receptor phosphorylation (6, 43). Both the TCR and CD4 are associated with nonreceptor tyrosine kinases that become activated after receptor ligation. This leads to activation of a range of intracellular molecules including PKC. We have recently provided evidence that PKC-mediated TCR internalization involves recognition of the TCR subunit CD3 $\gamma$  as a substrate for PKC with subsequent phosphorylation of CD3 $\gamma$  serine 126 (S126). In this process, basic amino acids surrounding S126 are important (7). Whether the phosphorylated S126 is directly included in a motif recognized by receptor sorting molecules, or phosphorylation of S126 causes a conformational change that exposes the L-based motif remained to be determined.

In the present study, we show that AP-1 and AP-2 bind the CD3 $\gamma$  L-based motif. Furthermore, we demonstrate that this motif includes the acidic amino acid, aspartic acid 127 (D127), and we provide evidence indicating that phosphorylation of CD3 $\gamma$  S126 in the context of the complete TCR induces a conformational change that exposes the DxxxLL sequence as one united motif for AP binding. The phosphorylated S126 is not directly included in the internalization motif. Thus, the DxxxLL sequence is an active internalization motif in monomeric CD4/CD3 $\gamma$  chimeras independently of S126 and S126 is dispensable for binding of AP to CD3 $\gamma$  peptides *in vitro*. Insertion or deletion of a single amino acid between D127 and L131 in the DxxxLL sequence completely abolished internalization of both the TCR and the CD4/CD3 $\gamma$  chimeras, and inhibited binding of AP-1 and AP-2 to CD3 $\gamma$  peptides, strongly indicating that the DxxxLL sequence is recognized as one united motif by AP. Glutamic acid could substitute for aspartic acid at position 127, whereas only leucine was accepted at position 131. At position 132, bulky hydrophobic amino acids other than leucine were accepted, i.e., leucine = isoleucine > methionine > phenylalanine.

## Materials and Methods

### Cells and Antibodies

Jurkat gamma negative (JGN) cells, a TCR cell surface negative variant of

the human T cell line Jurkat that synthesize no CD3 $\gamma$  (11) were cultured in RPMI 1640 medium supplemented with penicillin  $2 \times 10^5$  U/liter (Leo Pharmaceutical Products, Ballerup, Denmark), streptomycin 50  $\mu$ g/liter (Merck, Darmstadt, Germany), and 10% (vol/vol) FCS (Life Technologies, Paisley, UK) at 37°C in 5% CO<sub>2</sub>. UCHT1 mouse mAb directed against human CD3 $\epsilon$  was obtained purified, and phycoerythrin (PE) conjugated from DAKOPATTS A/S (Glostrup, Denmark). Anti- $\alpha$ - (100/2),  $\beta$ - (100/1), and  $\gamma$ -adaptin (100/3) mAb were from Sigma Chemical Co. (St. Louis, MO). The rat anti-mouse CD4 mAb L3T4 was obtained purified and PE conjugated from PharMingen (San Diego, CA). The anti-TCR mAb F101.01 was produced in our own laboratory (12). Rabbit anti-rat Ig was obtained from DAKOPATTS A/S, and FITC-conjugated F(ab)<sub>2</sub> fragments of donkey anti-rat Ig was obtained from Jackson Immunoresearch Laboratories, Inc. (West Grove, PA). The phorbol ester phorbol 12,13-dibutyrate (PDB) was from Sigma Chemical Co.

### Constructs, Transfection, and TCR Downregulation

All CD3 $\gamma$  mutations were constructed as previously described (6, 8) by the PCR using Vent DNA polymerase containing 3' to 5' proofreading exonuclease activity (New England Biolabs Inc., Beverly, MA) and the plasmid pJ6T3 $\gamma$ -2 (20) as template. Chimeric CD4/CD3 $\gamma$  (CD4/3-tS126), composed of the extracellular and transmembrane domains of mouse CD4 and a truncated cytoplasmic domain of human CD3 $\gamma$ , was produced using the plasmid pCD-L3T4.25 (25) as template, and the primer set CD4-up: 5'-CTCAAGTCTAGAACCATGTGCCGAGCCATCTCT; and CD4/3-t126: 5'-CTTGTGCAATTCTCAAGCTCGAGACTGGCGAACTCCATCCTGGACACAGCAGAGGATGCA by PCR. The PCR product was digested with XbaI and EcoRI, and subcloned into the expression vector pMH-Neo (14) to generate plasmid pMH-Neo-CD4/3-tS126. CD4/3-WT, CD4/3-SA, CD4/3-SDAA, CD4/3-SDAE, CD4/3-1A, and CD4/3-dT130 were produced using the plasmid pMH-Neo-CD4/3-tS126 as template, and the 5'-primer CD4-up and the 3'-primers: 5'-GTCCTTGAAT-TCTCACAACGAGTCTGCTTGTCTGAAGCGGAGACTGGAGAA-TCCATC, 5'-GTCCTTGAATTCACAACAGACTGCTGCTTGTCTCAGCAGCGGAGACTGGCGAACTCCATC, 5'-GTCCTTGAATTCACAACAGACTGGCGAACTCCATC, 5'-GTCCTTGAATTCACAACAGACTGGCGAACTCCATC, 5'-GTCCTTGAATTCACAACAGACTGGCGAACTCCATC, 5'-GTCCTTGAATTCACAACAGACTGGCGAACTCCATC, respectively. Mutations were confirmed by DNA sequencing. Transfections were performed using a Gene Pulser (Bio Rad Laboratories, Hercules, CA) at a setting of 270 V and 960 microfarad with 40  $\mu$ g of plasmid per  $2 \times 10^7$  cells. After 3–4 wk of selection, G418 resistant clones were expanded and maintained in medium without G418. For TCR downregulation, cells were adjusted to  $10^5$  cells/ml medium (RPMI 1640/10% FCS) and incubated at 37°C with various concentrations of phorbol ester. At the indicated time cells were transferred to ice-cold PBS containing 2% FCS and 0.1% NaN<sub>3</sub> and washed twice. The cells were stained directly with PE-conjugated UCHT1 and analyzed in a FACScan<sup>®</sup> flow cytometer (Becton and Dickinson, Co., Mountain View, CA). Mean fluorescence intensity (MFI) was recorded and used in the calculation of percent anti-CD3 binding: MFI of phorbol ester-treated cells, divided by MFI of untreated cells. For each construct, at least three different clones were analyzed.

### CD3 $\gamma$ Phosphorylation, Internalization of Chimeric CD4/CD3 $\gamma$ Receptors, and Intracellular Calcium

Phosphorylation assays were performed as previously described (6, 7). The phosphorylated CD3 $\gamma$  chain with a mol wt of 26–30 kD was coprecipitated with CD3 $\epsilon$  (20 kD) using the anti-CD3 $\epsilon$  mAb UCHT1. For each construct, at least two different clones were analyzed. To determine internalization of chimeric CD4/CD3 $\gamma$  receptors, cells were incubated in RPMI 1640 + 10% FCS at a cell density of  $2 \times 10^5$  cells per ml at 37° or 4°C with PE-conjugated anti-CD4 mAb. At the time indicated, aliquots of cell suspension were washed in ice-cold RPMI 1640 + 10% FCS and immediately treated with 300  $\mu$ l 0.5 M NaCl, 0.5 M acetic acid, pH 2.2 for 10 s. The acid-resistant fluorescence of the cells (representing internalized anti-CD4) was measured in the FACScan<sup>®</sup>. The percentage of internalized anti-CD4 to cell surface-bound anti-CD4 was subsequently calculated using the equation:  $HAR - CAR/CT$ . In this equation, *HAR* is the MFI of acid-treated cells incubated at 37°C; *CAR* is the MFI of acid-treated cells

incubated at 4°C, and CT is the MFI of untreated cells incubated at 4°C. For each construct at least three different clones were analyzed.

Intracellular calcium,  $[Ca^{2+}]_i$ , of cells was measured with the intracellular fluorescent indicator fura-2/AM (Sigma Chemical Co.) as previously described (17).

### Metabolic Labeling and Immunofluorescence Microscopy

Metabolic labeling studies were performed as previously described (8) using  $[^{35}S]$ methionine and  $[^{35}S]$ cysteine Promix™ (Amersham International, Little Chalfont, UK). Labeled cells were lysed in 1% NP-40 lysis buffer (20 mM Tris-HCl, pH 8.0, 1 mM MgCl<sub>2</sub>, 150 mM NaCl, 1 mM PMSF, 8 mM iodoacetamide, and 1% NP-40), precipitated with rat anti-mouse CD4 and rabbit anti-rat Ig, and subsequently analyzed by SDS-PAGE on 10% acrylamide gels under nonreducing conditions. Autoradiography of the dried gels was performed by using Hyperfilm-MP (Amersham International). <sup>14</sup>C-proteins from Amersham International were used as mol wt markers.

For immunofluorescence microscopy, cytospin preparations of the cells were fixed for 5 min in methanol at -20°C and then for 30 s in acetone at -20°C. The preparations were air-dried at room temperature for 20 h, and subsequently washed by immersion in PBS for 5 min. After incubation with donkey serum diluted 1:20 in PBS for 20 min, the preparations were incubated with rat anti-mouse CD4 (PharMingen) for 30 min, washed in PBS, incubated with FITC-conjugated F(ab)<sub>2</sub> fragments of donkey anti-rat IgG (Jackson ImmunoResearch Laboratories) for 30 min, washed in PBS, and subsequently inspected in a Leitz Dialux 20 microscope (Leica, Wetzlar, Germany).

### In Vitro Binding Studies Using CD3γ Peptides

Peptides corresponding to the membrane-proximal part of the CD3γ cytoplasmic tail from Q117 to L132, with a Q117 to cysteine mutation were obtained from Schafer-N (Copenhagen, Denmark) bound to vinyl-activated Sepharose 4B beads at a density of ~1–2 μmol/ml gel. The coupling procedure via the amino-terminal cysteine resulted in immobilization of monomeric peptides with freely exposed carboxy termini. To prepare T cell cytosol  $4 \times 10^8$  Jurkat cells were washed three times in cytosol buffer (25 mM HEPES, pH 7.0, 125 mM CH<sub>3</sub>COOK, 2.5 mM (CH<sub>3</sub>COO)<sub>2</sub>Mg, 1.0 mM DTT, 1 mg/ml glucose), and the resulting cell pellet was resuspended in an equal volume of cytosol buffer with inhibitors added (0.75 μM aprotinin, 10 μM leupeptin, 3 μM pepstatin A, 1 mM PMSF, 0.4 mM EDTA). The cell suspension was frozen in liquid nitrogen, thawed on ice, and drawn five times through a 21-gauge syringe. After centrifugation for 30 min at 20,000 g, 4°C, the cytosol was transferred to new tubes and then kept at -80°C until use. The protein concentration in the cytosol preparations was 15–20 mg/ml. Beads were incubated with T cell cytosol for 2 h at 37°C, washed three or six times in PBS at 4°C, and bound material was eluted by boiling the beads in Laemmli sample buffer with 5% 2-ME. After SDS-PAGE, the eluted material was transferred to nitrocellulose-membranes, and immunoblottings were performed using anti-α-, anti-β-, or anti-γ-adaptin antibodies followed by peroxidase-conjugated, rabbit anti-mouse antibodies (DAKOPATTS A/S). Bound antibodies were visualized using enhanced chemiluminescence (ECL; Amersham).

## Results

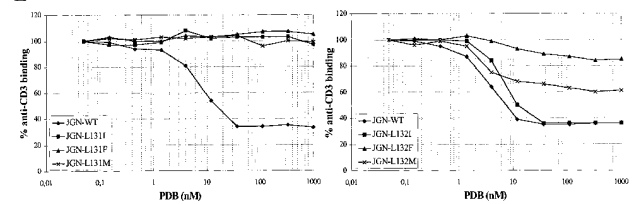
### Requirements to Residue 131 and 132

Only conservative variations of L-based sorting motifs composed of a leucine followed by another bulky hydrophobic amino acid have been identified (38). We have recently shown that phosphorylation of CD3γ S126 is required for PKC-mediated downregulation of the TCR (6). In addition to phosphorylation of S126, two leucines (L131 and L132), are required for TCR downregulation after PKC activation (6). These leucines are not CD3γ determinants for PKC as carboxyterminal truncations of the CD3γ cytoplasmic tail up to T130 do not affect PKC-mediated phosphorylation of CD3γ (6). To analyze which amino acid functioned in TCR internalization at position

A

Cell line	CD3γ cytoplasmic tail sequence	TCR down-regulation
JGN-WT	QDGVRSRAS DKQTLPLNDQ LYQPLKRDRE DQYSHLQGN LRRN	+++
JGN-L131I	-----I-----	-
JGN-L131F	-----F-----	-
JGN-L131M	-----M-----	-
JGN-L132I	-----I-----	+++
JGN-L132F	-----F-----	(+)
JGN-L132M	-----M-----	+

B



C

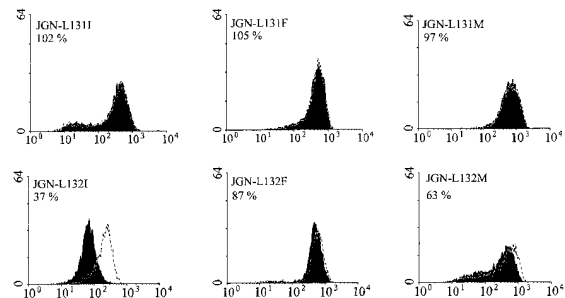


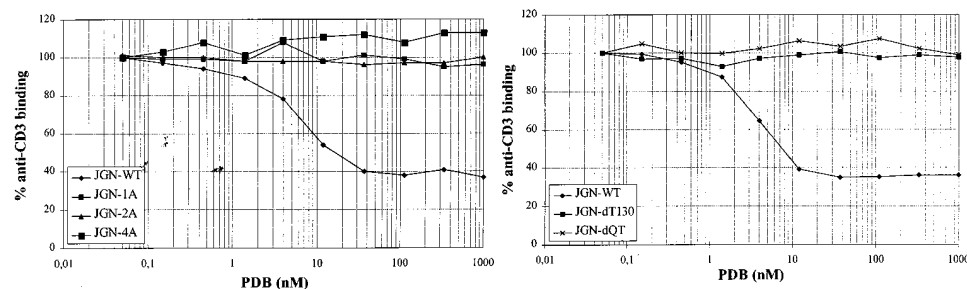
Figure 1. Requirements to residue 131 and 132. (A) Schematic representation of the amino acid sequences in the cytoplasmic tails of the CD3γ chains expressed in the indicated cell lines and a summation of the results from the TCR downregulation analyses. TCR downregulation was scored according to the percent anti-CD3 binding after incubation with PDB (110 nM) for 1 h: +++, 0–40% anti-CD3 binding; ++, 40–60% anti-CD3 binding; +, 60–80% anti-CD3 binding; (+), 80–95% anti-CD3 binding; -, >95% anti-CD3 binding. (B) Cells were incubated with different concentrations of PDB for 1 h and TCR downregulation was determined by staining with anti-CD3 mAb and flow cytometry comparing MFI of PDB-treated cells with MFI of untreated cells. (C) FACS® histograms of untreated cells (white, dotted line) and cells treated with 110 nM PDB (black) for 1 h. The cell line and the percent anti-CD3 binding after PDB treatment are given in the upper left corner of each histogram. The ordinate indicates the relative cell number. The abscissa indicates the fluorescence intensity in a logarithmic scale in arbitrary units. MFI of the cell lines stained with irrelevant mAb varied between two and five arbitrary units (data not shown).

131 and 132 in the cytoplasmic tail of CD3γ, constructs were made in which isoleucine, phenylalanine, or methionine substituted for L131 or L132 (Fig. 1 A). These constructs were separately transfected into the CD3γ negative T cell line JGN which upon transfection with CD3γ becomes TCR positive (11). TCR positive clones were isolated, and their ability to internalize the TCR after PKC activation was determined. The requirements to position 131 were very strict. Of the analyzed amino acids, only leucine was accepted at position 131 (Fig. 1, B and C). In contrast, TCR internalization seemed to be less restricted in its requirements to the amino acid at position 132. Thus, isoleucine functioned as well as leucine at this position. Methionine and phenylalanine also functioned at this position but with decreasing efficiency (Fig. 1, B and C).

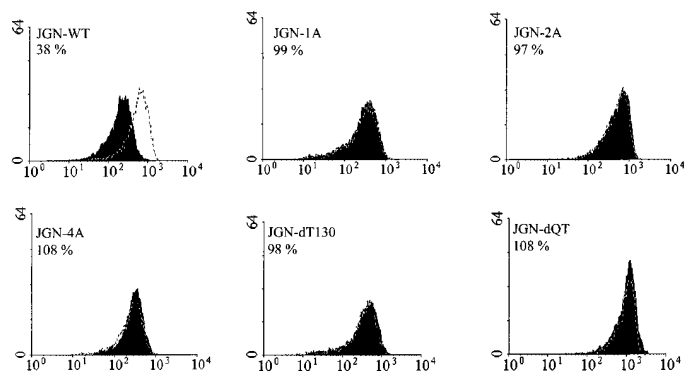
A

Cell line	CD3 $\gamma$ cytoplasmic tail sequence	CD3 $\gamma$ phosphorylation	TCR down-regulation
JGN-WT	QDGVRSRAS DKQTLLPNDQ LYQPLKDRED DQYSHLQGNQ LRRN	+	+++
JGN-1A	-----AQTLPLND QLYQPLKDRE DDQYSHLQGN QLRRN	+	-
JGN-2A	-----AAQTLLPN DQLYQPLKDR EDDQYSHLQG NQLRRN	+	-
JGN-4A	-----AAAQTLPL PNDQLYQPLK DREDDQYSHL QGNQLRRN	+	-
JGN-dT130	-----QLLPNDQL YQPLKDREDD QYSHLQGNQL RRN	+	-
JGN-dQT	-----LLPNDQLY QPLKDREDDQ YSHLQGNQLR RN	+	-

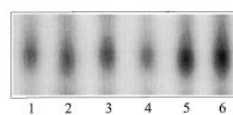
B



C



D



mAb varied between two and five arbitrary units (data not shown). (D) Phosphorylation analyses of CD3 $\gamma$  from JGN-WT (lane 1), JGN-1A (lane 2), JGN-2A (lane 3), JGN-4A (lane 4), JGN-dT130 (lane 5), and JGN-dQT (lane 6) cells.

### Insertion or Deletion of a Single Amino Acid Between SD and LL Abolishes TCR Internalization

We have previously shown that in addition to phosphorylation of S126 and the presence of L131 and L132, PKC-mediated TCR internalization is dependent on D127 (7). As S126 phosphorylation is not dependent on D127, this indicated that D127 may be directly included in the L-based receptor sorting motif. If the pSDxxxLL sequence is recognized as one motif by molecules involved in internalization it would be expected that the spacing between SD and LL is very important. To investigate whether the spacing of S126D127 relative to L131L132 influenced TCR internalization, constructs in which one or more amino acids were inserted or deleted between D127 and L131 were transfected into JGN cells (Fig. 2 A). TCR-positive clones were isolated and their ability to internalize the TCR after PKC activation was determined. Insertion or deletion of a single amino acid completely abolished TCR internalization (Fig. 2, B and C), although CD3 $\gamma$  phosphorylation was intact (Fig. 2 D). Taken together, these results strongly indicated that either S126 plus D127, or D127 alone, is directly included in the L-based sorting motif of CD3 $\gamma$ .

Figure 2. Insertion and deletion of amino acids between D127 and L131. (A) Schematic representation of the amino acid sequences in the cytoplasmic tails of the CD3 $\gamma$  chains expressed in the indicated cell lines and a summation of the results from the TCR downregulation and CD3 $\gamma$  phosphorylation analyses. TCR downregulation were scored as described in the legend to Fig. 1. (B) Cells were incubated with different concentrations of PDB for 1 h, and TCR downregulation was determined by staining with anti-CD3 mAb and flow cytometry comparing MFI of PDB treated cells with MFI of untreated cells. (C) FACS<sup>®</sup> histograms of untreated cells (white, dotted line) and cells treated with 110 nM PDB (black) for 1 h. The cell line and the percent anti-CD3 binding following PDB treatment are given in the upper left corner of each histogram. The ordinate indicates the relative cell number. The abscissa indicates the fluorescence intensity in a logarithmic scale in arbitrary units. MFI of the cell lines stained with irrelevant

### In Vitro Binding of AP to CD3 $\gamma$ Peptides

To test whether the cytoplasmic tail of CD3 $\gamma$  represented a binding motif for AP complexes, peptides corresponding to the membrane-proximal part of the CD3 $\gamma$  cytoplasmic tail from glutamine 117 (Q117) to L132, with a Q117 to cysteine mutation, were synthesized and immobilized on Sepharose beads. The coupling procedure resulted in immobilization of monomeric peptides with freely exposed carboxy termini. Thus, the orientation of the immobilized peptides mimicked that of the CD3 $\gamma$  cytoplasmic tail in vivo. Beads were incubated with T cell cytosol, washed three times in PBS, and bound material was eluted. After SDS-PAGE, the eluted material was transferred to nitrocellulose membranes, and immunoblottings were performed using anti- $\alpha$ -, anti- $\beta$ -, or anti- $\gamma$ -adaptin antibodies. Peptides representing the wild-type sequence of CD3 $\gamma$  (GAM-WT) precipitated  $\alpha$ -,  $\beta$ -, and  $\gamma$ -adaptin, whereas peptides in which alanines substituted for the leucines corresponding to L131 and L132 (GAM-LLAA) did not precipitate  $\alpha$ - and  $\beta$ -adaptin, and only weakly precipitated  $\gamma$ -adaptin (Fig. 3 A). Increasing the number of washes of the beads from three to six reduced the amount of  $\gamma$ -adaptin precipitated with the GAM-LLAA beads, whereas the

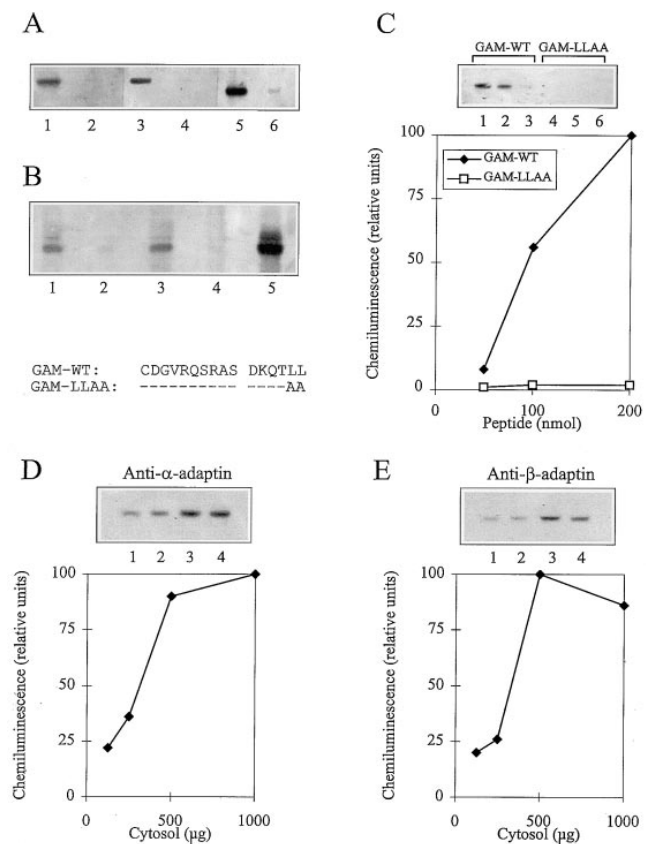


**Figure 3.** In vitro binding of AP to CD3 $\gamma$  peptides. (A) Western blots of material from T cell cytosol bound by beads coated with GAM-WT (lanes 1, 3, and 5) and GAM-LLAA (lanes 2, 4, and 6) peptides, and blotted with anti- $\alpha$ -adaptin (lanes 1 and 2), anti- $\beta$ -adaptin (lanes 3 and 4), and anti- $\gamma$ -adaptin (lanes 5 and 6) antibodies. The amino acid sequences of the GAM-WT and GAM-LLAA peptides are given below Fig. 3 B. (B) Western blot of material from T cell cytosol bound by beads coated with GAM-WT (lanes 1 and 3) and GAM-LLAA (lanes 2 and 4) peptides with unprocessed T cell cytosol in lane 5 blotted with a mixture of anti- $\alpha$ -adaptin and anti- $\gamma$ -adaptin antibodies. The beads were either washed three times (lanes 1 and 2) or six times (lanes 3 and 4) before the bound material was eluted. (C) Western blot of material from T cell cytosol bound by beads coated with GAM-WT (lanes 1–3) and GAM-LLAA (lanes 4–6) peptides blotted with anti- $\alpha$ -adaptin antibody. The amount of beads used represented 200 (lanes 1 and 4), 100 (lanes 2 and 5), and 50 (lanes 3 and 6) nmol bound CD3 $\gamma$  peptide. A plot of the bands quantitated by densitometry is given below. The bands are normalized to the band obtained with 200 nmol GAM-WT peptide. (D) Western blot of material from T cell cytosol bound by beads coated with GAM-WT peptides and blotted with the anti- $\alpha$ -adaptin antibody. Increasing amounts (125 [lane 1], 250 [lane 2], 500 [lane 3], and 1,000 [lane 4]  $\mu$ g) of T cell cytosol were used. The amount of beads was constant and represented 200 nmol bound CD3 $\gamma$  peptide. A plot of the bands quantitated by densitometry is given below. The bands are normalized to the band obtained with 1,000  $\mu$ g T cell cytosol. (E) Western blot of material from T cell cytosol bound by beads coated with GAM-WT peptides and blotted with the anti- $\beta$ -adaptin antibody. Increasing amounts (125 [lane 1], 250 [lane 2], 500 [lane 3], and 1,000 [lane 4]  $\mu$ g) of T cell cytosol were used. The amount of beads was constant and represented 200 nmol bound CD3 $\gamma$  peptide. A plot of the bands quantitated by densitometry is given below. The bands are normalized to the band obtained with 500  $\mu$ g T cell cytosol.

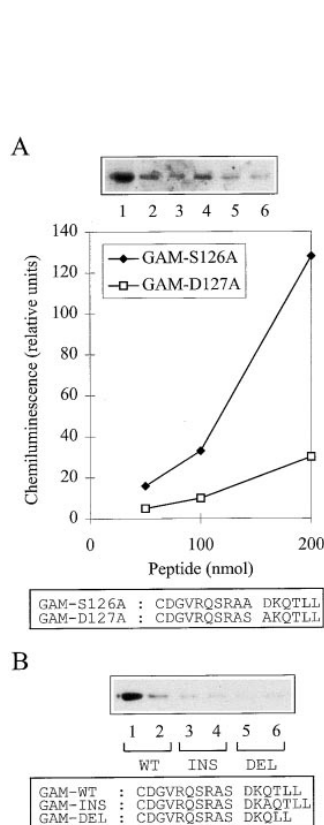


**Figure 4.** Binding of AP to mutated CD3 $\gamma$  peptides. (A) Western blot of material from T cell cytosol bound by beads coated with GAM-S126A (lanes 1–3) and GAM-D127A (lanes 4–6) peptides blotted with the anti- $\alpha$ -adaptin antibody. The amount of beads used represented 200 (lanes 1 and 4), 100 (lanes 2 and 5), and 50 (lanes 3 and 6) nmol bound CD3 $\gamma$  peptide. A plot of the bands quantitated by densitometry is given below. The bands are normalized to the band obtained with 200 nmol GAM-WT peptide. (B) Western blot of material from T cell cytosol bound by beads coated with GAM-WT (lanes 1 and 2), GAM-INS (lanes 3 and 4), and GAM-DEL (lanes 5 and 6) peptides blotted with the anti- $\alpha$ -adaptin antibody. The amount of beads used represented 200 (lanes 1, 3, and 5) and 100 (lanes 2, 4, and 6) nmol bound CD3 $\gamma$  peptide.

amount of  $\gamma$ -adaptin precipitated with GAM-WT was not significantly reduced (Fig. 3 B). Titration of beads and cytosol demonstrated that GAM-WT beads precipitated  $\alpha$ -,  $\beta$ -, and  $\gamma$ -adaptin in parallel (Fig. 3, C–E, and data not shown). The observation that GAM-WT bound APs although the peptide was not phosphorylated, indicated either that the peptide became phosphorylated during the incubation with cytosol or that phosphorylation of serine corresponding to CD3 $\gamma$  S126 was not required for in vitro binding. To analyze the role of serine in AP binding, peptides in which alanine substituted for serine (GAM-S126A) were produced. These peptides bound AP as efficiently as GAM-WT, suggesting that S126 is not required for AP binding (Fig. 4 A). In contrast, peptides in which alanine substituted for aspartic acid corresponding to CD3 $\gamma$  D127 bound AP less efficiently, suggesting that D127 is required for optimal AP binding (Fig. 4 A). Likewise, peptides in which one amino acid was inserted (GAM-INS) or deleted (GAM-DEL) between the aspartic acid and leucine corresponding to CD3 $\gamma$  D127 and L131, respectively, bound AP less efficiently than the GAM-WT and GAM-S126A peptides (Fig. 4 B).

#### *The DxxxLL Sequence Acts as an Active Receptor Sorting Motif in CD4/CD3 $\gamma$ Chimeras Independently of S126*

Combining the observations that phosphorylation of CD3 $\gamma$  S126 was required for TCR internalization and that S126 was dispensable for AP binding in vitro, suggested that the role of S126 phosphorylation in T cells was to induce a conformational change that exposed the DxxxLL

motif for adaptor binding. As the TCR is a multimeric receptor composed of at least eight chains (all possessing cytoplasmic tails), it is possible that the DxxxLL motif of CD3 $\gamma$  in the context of the complete TCR is not accessible in the nonphosphorylated state for molecules involved in internalization. This hypothesis implies that the DxxxLL receptor sorting motif may be active in monomeric receptors independently of serine. Accordingly, constructs coding for the extracellular and transmembrane parts of CD4, and the membrane-proximal part of the CD3 $\gamma$  cytoplasmic tail from Q117 to L132 (with various mutations) were transfected into JGN cells (Fig. 5 A). As an L-based motif negative control, the CD4/3-tS126 construct (coding for the extracellular and transmembrane part of CD4, and the membrane-proximal part of CD3 $\gamma$  from Q117 to A125) was transfected into JGN cells (Fig. 5 A). If the DxxxLL motifs in the CD4/3-WT and CD4/3-SA chimeras and the ExxxLL motif in the CD4/3-SDAE chimera were active

independently of the presence and/or phosphorylation of S126, then it would be expected that only small amounts of the chimeras were expressed at the cell surface, and that these molecules were quickly internalized. Likewise, if the aspartic acid was required in an active sorting motif, the CD4/3-SDAA chimeric molecules would be expected to be highly expressed at the cell surface and to have a low turnover rate like the CD4/3-tS126 chimeras. G418-resistant clones were isolated and analyzed for cell surface expression of the chimeric molecules by FACS<sup>®</sup> analysis using an anti-CD4 mAb. Clones transfected with CD4/3-WT, CD4/3-SA, and CD4/3-SDAE only weakly expressed the chimeric molecules at the cell surface. In contrast, clones transfected with CD4/3-tS126 and CD4/3-SDAA highly expressed the chimeric molecules at the cell surface (Fig. 5 B, upper row). Pulse-chase metabolic labeling demonstrated that the amounts of chimeric molecules produced in the transfectants were comparable, and that the

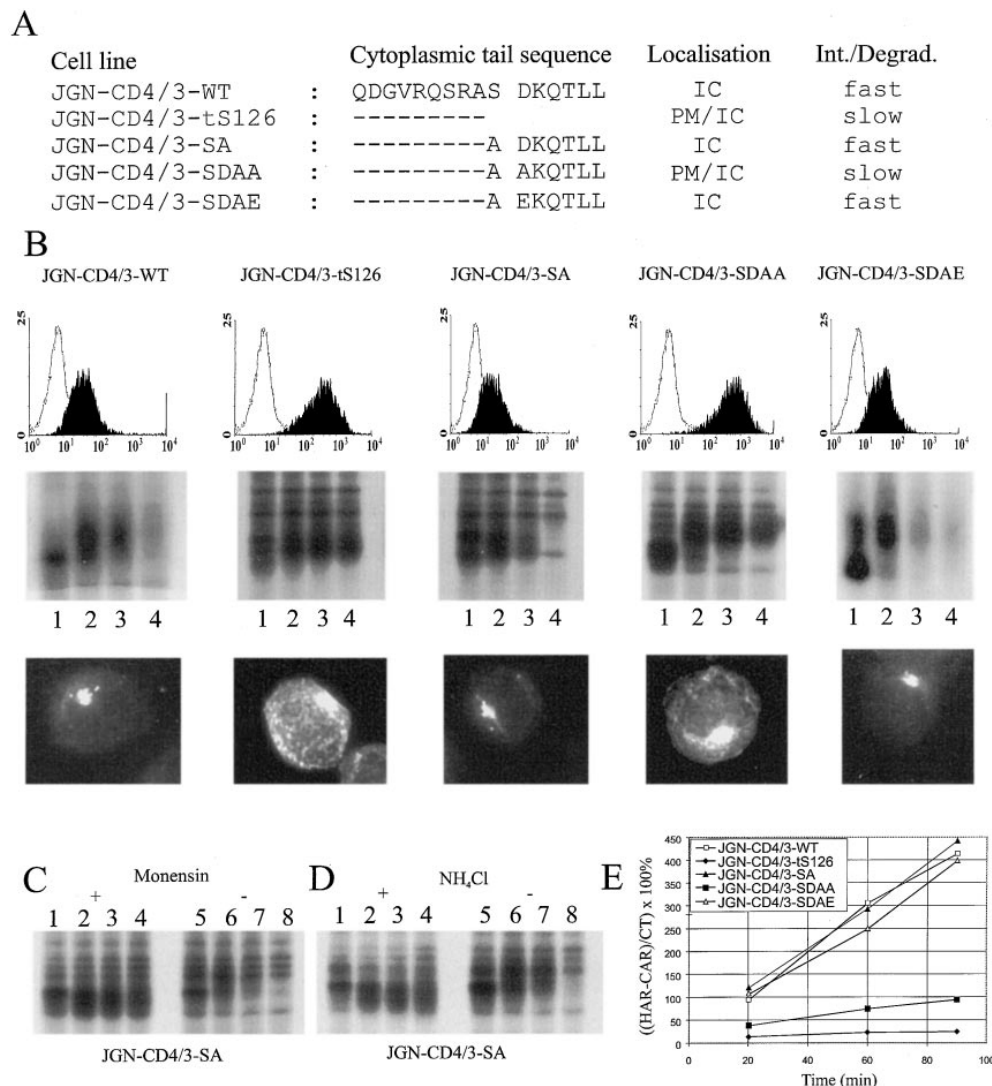


**Figure 5.** The DxxxLL sequence is an active sorting motif in CD4/CD3 $\gamma$  chimeras. (A) Schematic representation of the amino acid sequences in the cytoplasmic tails of the CD4/CD3 $\gamma$  chimeras expressed in the indicated cell lines and a summation of the results obtained from FACS<sup>®</sup> analysis, immunofluorescence microscopy, pulse-chase metabolic labeling, and internalization experiments. IC, intracellular; PM, plasma membrane. (B) The FACS<sup>®</sup> profile (first row), the results from pulse-chase metabolic labeling studies (second row), and the results from immunofluorescence microscopy analyses (third row) are shown for each cell line. The name of the relevant cell line is given at the top of each column. The FACS<sup>®</sup> profiles show the relevant cell line in black and the JGN cell line in white. For pulse-chase metabolic labeling, cells were pulsed for 30 min (lane 1) and chased for 1 (lane 2), 2 (lane 3), and 4 (lane 4) h. (C) Pulse-chase metabolic labeling of JGN-CD4/3-SA cells as in B, in the presence or absence of monensin or (D) ammonium chloride. (E) Internalization of anti-CD4 antibodies by chimeric receptors. The percentage of internalized anti-CD4 to cell surface bound anti-CD4 was calculated as described in Materials and Methods.

CD4/3-WT, CD4/3-SA, and CD4/3-SDAE molecules were quickly degraded with almost no labeled molecules left after a 4-h pulse, whereas the CD4/3-tS126 and CD4/3-SDAA molecules were far more stable (Fig. 5 B, middle row). Furthermore, immunofluorescence microscopy of fixed and permeabilized cells showed a predominant intracellular localization of CD4/3-WT, CD4/3-SA, and CD4/3-SDAE molecules clustered in few large vesicles. In contrast, CD4/3-tS126 and CD4/3-SDAA molecules were found both at the plasma membrane and intracellularly (Fig. 5 B, lower row). Several lines of evidence pointed to endosomes/lysosomes as the likely site of degradation of the CD4/3-WT, CD4/3-SA, and CD4/3-SDAE molecules. First, when protein transport through the Golgi apparatus was inhibited by monensin, degradation was blocked (Fig. 5 C). Second, the degradation destroyed fully processed molecules, pointing to a site of degradation beyond the Golgi apparatus (Fig. 5 B, middle row). Finally, ammonium chloride, known to inhibit lysosomal degradation, inhibited degradation (Fig. 5 D).

Whether the CD4/3-WT, CD4/3-SA, and CD4/3-SDAE molecules were transported directly from the TGN to endosomes/lysosomes for degradation or were transported via the plasma membrane was studied next. Cells were incubated with PE-conjugated, anti-CD4 mAb for 20, 60, or 90 min at 37°C. Subsequently, the cells were washed and mAb was stripped of the cell surface by incubating the cells in low pH buffer. The amount of acid-resistant mAb representing receptor-mediated, internalized mAb was subsequently determined by FACS<sup>®</sup> analysis. Cells expressing CD4/3-WT, CD4/3-SA, or CD4/3-SDAE molecules had a high intake rate of anti-CD4 mAb, whereas cells expressing CD4/3-SDAA or CD4/3-tS126 molecules had a low mAb intake rate (Fig. 5 E). This indicated that at least a fraction of the CD4/3-WT, CD4/3-SA, and CD4/3-SDAE molecules were transported via the plasma membrane.

### Insertion or Deletion of a Single Amino Acid in the DxxxLL Motif Reduces the Internalization and Degradation Rate of Chimeric Molecules

If the DxxxLL sequence was recognized as one motif for AP binding in the chimeric CD4/CD3 $\gamma$  molecules, as suggested by the TCR and peptide experiments, it would be expected that insertion or deletion of amino acids between D127 and L131 would reduce the internalization rate and degradation of the chimeras. To test this, chimeric CD4/CD3 $\gamma$  constructs in which one amino acid was inserted or deleted between D127 and L131 were transfected into JGN cells (Fig. 6 A). G418-resistant clones were isolated and examined for cell surface expression of the chimeras by FACS<sup>®</sup> analysis using an anti-CD4 mAb. Both CD4/3-1A and CD4/3-dT130 molecules were highly expressed at the cell surface of the transfectants (Fig. 6 B). Pulse-chase metabolic labeling showed that, in contrast to CD4/3-SA molecules, CD4/3-1A and CD4/3-dT130 were stable for at least 4 h (Fig. 6 C). Incubation with PE-conjugated anti-CD4 mAb at 37°C demonstrated that cells expressing CD4/3-1A or CD4/3-dT130 molecules had a lower intake rate of mAb as compared to cells expressing CD4/3-SA (Fig. 6, D and E). Furthermore, immunofluorescence microscopy showed that the CD4/3-1A and CD4/3-dT130 molecules were localized both at the plasma membrane and intracellularly (data not shown).

### Exposure of the DxxxLL Motif in the TCR Results in an Impairment of TCR Signaling

To test whether TCR downregulation caused by the exposure of the DxxxLL motif had any influence on mAb-induced TCR activation, JGN-WT and JGN-L131F cells were incubated with different concentrations of PDB for 30 min and subsequently divided in two parts. One part was analyzed for TCR expression by FACS<sup>®</sup> and the other part was analyzed for intracellular calcium [Ca<sup>2+</sup>]<sub>i</sub> mobili-

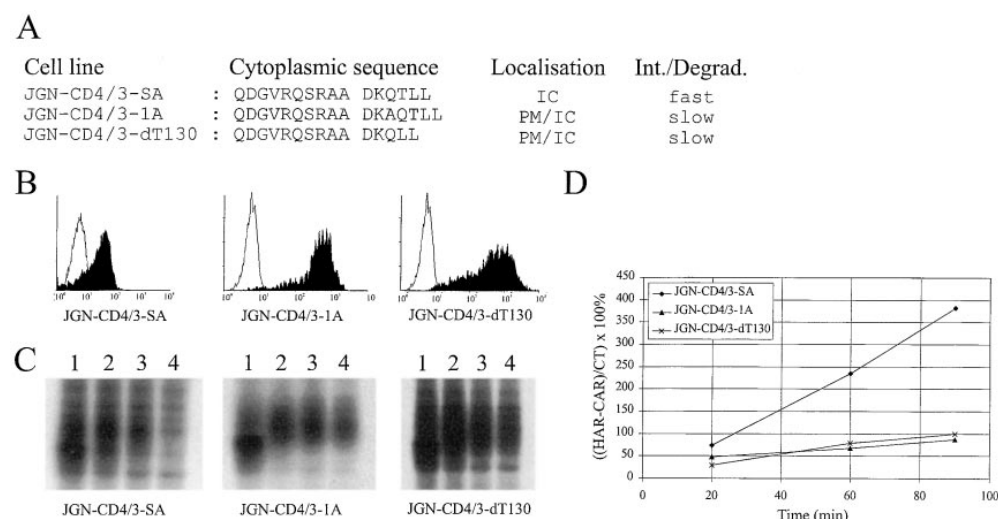
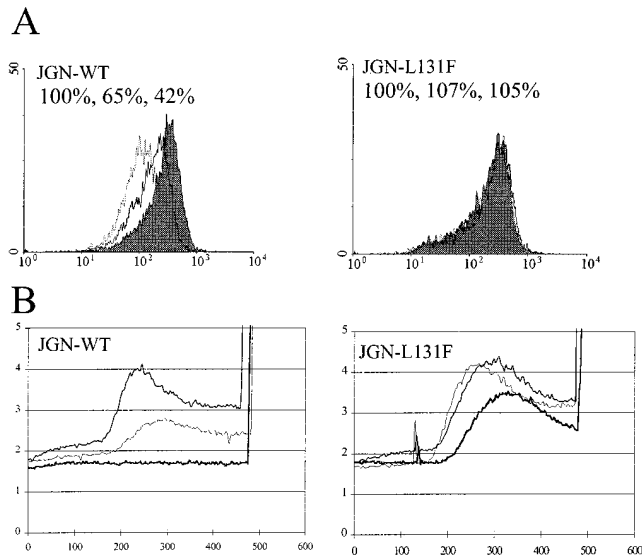


Figure 6. Internalization and degradation is reduced by insertion or deletion of amino acids in the DxxxLL motif. (A) Schematic representation of the amino acid sequences in the cytoplasmic tails of the CD4/CD3 $\gamma$  chimeras expressed in the indicated cell lines, and a summation of the results obtained from FACS<sup>®</sup> analysis, immunofluorescence microscopy, pulse-chase metabolic labeling, and internalization experiments. IC, intracellular; PM, plasma membrane. (B) The FACS<sup>®</sup> profiles show the indicated cell line in black and the JGN cell line in white. (C) Pulse-chase metabolic labeling. JGN-CD4/3-SA, JGN-CD4/3-1A, and JGN-CD4/3-dT130 cells were pulsed for 30 min (lane 1) and chased for 1 (lane 2), 2 (lane 3), and 4 (lane 4) h. (D) Internalization of anti-CD4 antibodies by chimeric receptors. The percentage of internalized anti-CD4 to cell surface bound anti-CD4 was calculated as described in Materials and Methods.

Labeling. JGN-CD4/3-SA, JGN-CD4/3-1A, and JGN-CD4/3-dT130 cells were pulsed for 30 min (lane 1) and chased for 1 (lane 2), 2 (lane 3), and 4 (lane 4) h. (D) Internalization of anti-CD4 antibodies by chimeric receptors. The percentage of internalized anti-CD4 to cell surface bound anti-CD4 was calculated as described in Materials and Methods.



**Figure 7.** Exposure of the DxxxLL motif in the TCR results in an impairment of TCR signaling. (A) FACS<sup>®</sup> profiles of JGN-WT and JGN-L131F cells incubated without PDB (*grey*), with 12 nM PDB (*bold line*), or with 110 nM PDB (*dotted line*) for 30 min. The ordinate indicates the relative cell number. The abscissa indicates the fluorescence intensity in a logarithmic scale in arbitrary units. The cell line and the percent anti-CD3 binding after treatment without PDB and with 12 and 110 nM PDB are given in the upper left corner of each histogram (B)  $[Ca^{2+}]_i$  measurements. After incubation of JGN-WT and JGN-L131F cells without PDB (*regular line*), with 12 nM PDB (*thin line*), or with 110 nM PDB (*thick line*) for 30 min, the cells were treated with the anti-TCR antibody F101.01 at 120 s, and subsequently with ionophore- $Ca^{2+}$  salt at 480 s. The ratio of fura-2/AM fluorescence at 340 nm to that at 380 nm was recorded and is indicated by the ordinate in arbitrary units. The abscissa indicates the time in seconds. The cell line is given in the upper left corner of each histogram.

zation after stimulation with suboptimal doses of the anti-TCR mAb F101.01 (12). TCR downregulation correlated with an impairment to mobilize  $[Ca^{2+}]_i$  in JGN-WT cells (Fig. 7). In contrast, incubation of JGN-L131F cells with PDB did not induce TCR downregulation and had only a minor inhibitory effects on F101.01-induced  $[Ca^{2+}]_i$  mobilization (Fig. 7).

## Discussion

Downregulation of receptors after receptor activation is a general phenomenon observed for a broad range of receptors (26). Recently, L-based motifs have been found to play an important role in internalization and sorting of several receptors of the immune system. Thus, the TCR (CD3 $\gamma$  and CD3 $\delta$ ) (6, 23), CD4 (43), the MHC class II-associated invariant chain (Ii) (34), gp130 (9), and CD44 (41) all contain L-based sorting motifs. In general, receptor downregulation is probably an important method by which a cell, after receptor signaling, attenuates its response to ligand stimulation and thereby protects itself from excessive signaling. Several mitogenic receptors with tyrosine kinase activity have oncogenic potential and the importance of tyrosine kinase receptor desensitization has

been shown by analyzing mutated epidermal growth factor receptors (EGFR). Stimulation with low concentrations of ligand leads to neoplastic transformation of cells expressing desensitization defective EGFR but not of cells expressing wild-type EGFR (28, 55). The physiological role of TCR downregulation mediated by the CD3 $\gamma$  phosphorylation-dependent, L-based sorting motif is still unknown. In addition, to protect the T cell from excessive signaling, it is likely that a strict regulation of this central receptor of the specific immune system is important both in the initial steps of T cell activation (49, 50) and in tolerance induction (1). This is supported by the present observation that TCR downregulation after PKC activation abolished suboptimal stimulation with anti-TCR mAb as measured by mobilization of  $[Ca^{2+}]_i$ .

In contrast to nutritive receptors that generally are constitutively internalized, rapid and efficient internalization via clathrin-coated pits and vesicles of signaling receptors (e.g., the TCR and EGFR) generally occurs only after ligand binding and receptor activation. One of the hallmarks of clathrin-coated vesicles is their selectivity. Certain membrane receptors are very efficiently concentrated in clathrin-coated vesicles, and in most cases this property has been correlated with the presence of a Y-based internalization signal in the cytoplasmic tail of the receptor (for reviews see references 48, 53). The mechanism by which activated receptors with Y-based internalization motifs are concentrated in clathrin-coated vesicles is not fully understood, although binding of AP-2 to the Y-based motifs may be involved (2, 13, 30–32, 44, 45). Phosphorylation of the tyrosine can probably be excluded as part of the mechanism, as phenylalanine sometimes can substitute for tyrosine (53). In contrast, some L-based motifs (e.g., CD3 $\gamma$ , CD4, and to some extent gp130) are dependent on serine phosphorylation, whereas others (e.g., Ii and CD44) are independent. We have previously shown that the L-based internalization motif in context of the complete TCR is strictly regulated by S126 phosphorylation (6). Taken together with the present observation that the DxxxLL motif was active in the CD4/CD3 $\gamma$  chimeras independently of serine, this suggested that the DxxxLL motif is most likely not accessible for the internalization machinery in the context of the complete TCR and that phosphorylation of S126 serves to induce a conformational change in the TCR that makes the DxxxLL motif accessible for the internalization machinery.

The molecular mechanisms involved in the sorting of receptors with L-based sorting motifs are still not fully known but seem to be highly specific. Only conservative variations (leucine plus another bulky hydrophobic amino acid) of L-based sorting motifs have been identified (38). For CD3 $\gamma$ , we found that at position 131 only leucine was accepted, whereas the requirements to position 132 were more relaxed (i.e., leucine = isoleucine > methionine > phenylalanine). This is in agreement with the presence of either LL, LI, or LM in the CD3 $\gamma$  and CD3 $\delta$  L-based motifs from different species (Table I). These results suggest that L-based motifs found in different receptors follow a common pattern and are recognized by the same or very homologous molecules.

It has not been clear whether the L-based sequence per se constitutes a complete targeting motif or additional res-



Table I. CD3 Leucine-based Motifs from Different Species

Species	Sequence
$\gamma/\delta$ frog	SDKQNLL
$\gamma/\delta$ chicken	SDRQNLI
$\gamma$ human	SDKQTLL
$\gamma$ mouse	SDKQTLL
$\gamma$ rat	SDKQTLL
$\gamma$ sheep	SDKQTLL
$\delta$ human	ADTQALL
$\delta$ mouse	AEVQALL
$\delta$ rat	VDTQVLL
$\delta$ sheep	ADTQVLM

Amino acid sequences of the L-based internalization motifs from frog CD3 $\gamma/\delta$  (These data are available from GenBank/EMBL/DDGI under accession number U78290), chicken CD3 $\gamma/\delta$  (3), human CD3 $\gamma$  (20), mouse CD3 $\gamma$  (21), rat CD3 $\gamma$  (24), sheep CD3 $\gamma$  (16), human CD3 $\delta$  (51), mouse CD3 $\delta$  (52), rat CD3 $\delta$  (5), and sheep CD3 $\delta$  (16).

idues are included in the motif. Recent studies of the Ii have indicated that sorting of Ii, in addition to L-based sequences, depends on an acidic amino acid positioned four or five residues amino terminal to the motif (29, 35). Furthermore, we have shown that CD3 $\gamma$  D127 is absolutely required for PKC-mediated TCR internalization although it is dispensable for S126 phosphorylation (7). The present study of the CD4/CD3 $\gamma$  chimeras demonstrated that a glutamic acid versus an alanine substitution for aspartic acid was accepted at position 127, which supports the suggestion that an acidic amino acid is included in L-based motifs. Interestingly, a phosphorylated serine could also substitute for aspartic acid or glutamic acid at position 127 in the CD4/CD3 $\gamma$  chimeras (Geisler, C., unpublished data). Furthermore, the results obtained by insertion or deletion of amino acids between D127 and L131 in the DxxxLL sequence strongly indicated that the DxxxLL sequence was recognized as one motif. This is also supported by the conserved D/ExxxLL/I/M sequences found in CD3 $\gamma$  and  $\delta$  from different species (Table I).

Although the D/ExxxLL/M motif found in different CD3 $\delta$  subunits works as a receptor sorting motif in chimeric receptors (the present study and reference 23), it is not preceded by a serine and it cannot substitute for the CD3 $\gamma$  motif in the context of the complete TCR (54). One role of this motif could be in TCR quality control by targeting incompletely assembled TCR complexes to the endosomes/lysosomes for degradation. In line with this, it has been demonstrated that TCR complexes lacking the  $\zeta$  chain are mainly transported to the lysosomes for degradation (46). These observations suggest that  $\zeta$  normally cover the L-based TCR internalization motifs, and this could explain why only completely assembled TCR are allowed to be normally expressed at the T cell surface.

Binding studies with peptides, representing the cytoplasmic tail of CD3 $\gamma$ , suggested that the DxxxLL motif was recognized by both AP-2 and AP-1. From these results we could not determine which subunit of the AP complexes was responsible for binding. Furthermore, the possibility that AP-DxxxLL binding was mediated by a third unidentified molecule could not be excluded. A recent study using the yeast two-hybrid system demonstrated a direct interaction of Y-based sorting motifs and the  $\mu$ 1 and  $\mu$ 2

chains but failed to detect any interaction between these chains and the CD3 $\gamma$  DKQTLL motif (31). This suggests that the  $\mu$ 1 and  $\mu$ 2 chains are not involved in binding to L-based sorting motifs, however, an alternative explanation could be that  $\mu$ 1 and  $\mu$ 2 are involved in binding, but only when found in the context of the complete AP complex. Although such in vitro experiments should be interpreted with caution, a much stronger binding of AP to GAM-WT compared to GAM-LLAA peptides was observed. The observation that S126 was dispensable for AP binding supported the results obtained in vivo, demonstrating that S126 was not required for internalization of the CD4/CD3 $\gamma$  chimeras. In addition, GAM-D127A peptides bound AP less efficiently than GAM-WT and GAM-S126A peptides, indicating that an acidic amino acid was required at this position for optimal AP binding in vitro. In line with this, in vivo studies of JGN-CD4/3-SDAA cells showed a reduced internalization rate of the chimeric molecules compared to JGN-CD4/3-SA cells. The finding that the DxxxLL motif bound both AP-2 and AP-1 complexes is in good agreement with the observation that L-based receptor sorting motifs are found both in receptors sorted from the TGN to endosomes/lysosomes (19, 23, 39) and in receptors internalized from the plasma membrane (4, 6, 9, 23, 43) and is furthermore supported by a recent study describing the in vitro binding of both AP-2 and AP-1 to L-based motifs by using surface plasmon resonance analysis (15).

From these results it may be suggested that receptors with L-based sorting motifs can be divided in three groups.

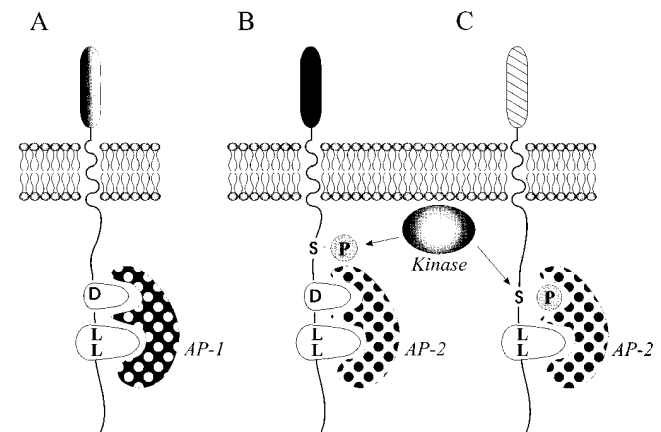


Figure 8. Three groups of receptors with L-based motifs. (A) In the first group of receptors, the L-based motifs are directly accessible and they are recognized by AP-1 at the TGN. This leads to sorting of the receptors from the TGN to the endosomes/lysosomes. (B) The second group represents multimeric plasma membrane receptors. In incompletely assembled receptors, the L-based motifs are accessible and recognized by AP-1 at the TGN, leading to degradation of nonfunctional receptors in the lysosomes. In completely assembled receptors, the L-based motif is not accessible for AP, and the receptors are transported to the plasma membrane. Only after receptor stimulation leading to kinase activation and receptor phosphorylation does the motif become accessible for AP-2 and the receptors are then internalized. (C) In the third group of receptors, a serine substitutes for the acidic amino acid in the L-based motif and the motif only becomes active after phosphorylation of this serine.

The first group includes receptors destined for the endosome/lysosome compartments. These receptors express a directly accessible L-based motif (e.g., Ii, the cation-dependent mannose 6-phosphate receptor, lysosomal integral membrane protein II, and the CD4/3-WT, -SA, and -SDAE chimeras). The accessible motif is recognized by AP-1 at the TGN and the majority of the receptors are sorted directly to the endosomes/lysosomes (Fig. 8 A). The second group includes multimeric plasma membrane receptors like the TCR. Here the L-based motif serves two functions: quality control; and receptor downregulation. In incompletely assembled receptors, the L-based motifs are accessible and recognized by AP-1 at the TGN leading to degradation of nonfunctional receptors in the lysosomes. In completely assembled receptors, the L-based motif is not accessible for AP and the receptors are transported to the plasma membrane. Only after receptor stimulation leading to kinase activation and receptor phosphorylation, the motif becomes accessible for AP-2 and the receptors are then internalized (Fig. 8 B). The third group includes monomeric plasma membrane receptors like CD4. In this group, a serine substitutes for the acidic amino acid in the L-based motif and the motif only becomes active after phosphorylation of this serine. This implies that receptors belonging to this group are transported from the Golgi apparatus to the plasma membrane, as the motif is not active at the TGN. Only after receptor stimulation at the plasma membrane leading to PKC activation and receptor phosphorylation, the motif becomes active leading to AP-2 binding and receptor internalization (Fig. 8 C).

We thank Dr. M.J. Crumpton for plasmid pJ6T3 $\gamma$ -2 and Dr. D.R. Littman for plasmid pCD-L3T4.25. The technical help of I.B. Olsen is gratefully acknowledged.

This work was supported by The Danish Cancer Society, The Novo Nordisk Foundation, The Danish Medical Research Council, The Danish Natural Science Research Council, Director Ib Henriksens Foundation, Gerda and Aage Haensch's Foundation, and Director Leo Nielsen and wife Karen Magrethe Nielsen Foundation for Medical Basic Research. J. Kastrup was a recipient of a scholarship from The Danish Cancer Society. J. Dietrich was a recipient of a Ph.D. scholarship from the University of Copenhagen. C. Geisler and N. Odum are members of The Biotechnology Centre for Cellular Communication.

Received for publication 24 March 1997 and in revised form 22 May 1997.

## References

- Arnold, B., G. Schonrich, and G.J. Hammerling. 1993. Multiple levels of peripheral tolerance. *Immunol. Today*. 14:12-14.
- Beltzer, J.P., and M. Spiess. 1991. In vitro binding of the asialoglycoprotein receptor to the beta adaptin of plasma membrane coated vesicles. *EMBO (Eur. Mol. Biol. Organ.) J.* 10:3735-3742.
- Bernot, A., and C. Auffray. 1991. Primary structure and ontogeny of an avian CD3 transcript. *Proc. Natl. Acad. Sci. USA*. 88:2550-2554.
- Bremnes, B., T. Madsen, M. Gedde-Dahl, and O. Bakke. 1994. An LI and ML motif in the cytoplasmic tail of the MHC-associated invariant chain mediate rapid internalization. *J. Cell. Sci.* 107:2021-2032.
- Davies, J.D., D. Mueller, D.B. Wilson, and D.P. Gold. 1990. Nucleotide sequence of a cDNA encoding the rat T3 delta chain. *Nucleic Acids Res.* 18:4617.
- Dietrich, J., X. Hou, A.K. Wegener, and C. Geisler. 1994. CD3 $\gamma$  contains a phosphoserine-dependent di-leucine motif involved in downregulation of the T cell receptor. *EMBO (Eur. Mol. Biol. Organ.) J.* 13:2156-2166.
- Dietrich, J., X. Hou, A.K. Wegener, L.O. Pedersen, N. Odum, and C. Geisler. 1996. Molecular characterization of the di-leucine based internalization motif of the T cell receptor. *J. Biol. Chem.* 271:11441-11448.
- Dietrich, J., A. Neisig, X. Hou, A.K. Wegener, M. Gajhede, and C. Geisler. 1996. Role of CD3 $\gamma$  in T cell receptor assembly. *J. Cell. Biol.* 132:299-310.
- Dittrich, E., C.R. Haft, L. Muys, P.C. Heinrich, and L. Graeve. 1996. A di-leucine motif and an upstream serine in the interleukin-6 (IL-6) signal transducer gp130 mediate ligand-induced endocytosis and downregulation of the IL-6 receptor. *J. Biol. Chem.* 271:5487-5494.
- Ferber, I., G. Schonrich, J. Schenkel, A.L. Mellor, G.J. Hammerling, and B. Arnold. 1994. Levels of peripheral T cell tolerance induced by different doses of tolerogen. *Science (Wash. DC)*. 263:674-676.
- Geisler, C. 1992. Failure to synthesize the CD3- $\gamma$  chain: Consequences for T cell antigen receptor assembly, processing, and expression. *J. Immunol.* 148:2437-2445.
- Geisler, C., T. Plesner, G. Pallesen, K. Skjodt, N. Odum, and J.K. Larsen. 1988. Characterization and expression of the human T cell receptor-T3 complex by monoclonal antibody F101.01. *Scand. J. Immunol.* 27:685-696.
- Glickman, J.N., E. Conibear, and B.M. Pearse. 1989. Specificity of binding of clathrin adaptors to signals on the mannose-6-phosphate/insulin-like growth factor II receptor. *EMBO (Eur. Mol. Biol. Organ.) J.* 8:1041-1047.
- Hahn, W.C., E. Menzin, T. Saito, R.N. Germain, and B.E. Bierer. 1993. The complete sequences of plasmids pFNeo and pMH-Neo: convenient expression vectors for high-level expression of eukaryotic genes in hematopoietic cell lines. *Gene (Amst.)*. 127:267-268.
- Heilker, R., U. Manning-Krieg, J.F. Zuber, and M. Spiess. 1996. In vitro binding of clathrin adaptors to sorting signals correlates with endocytosis and basolateral sorting. *EMBO (Eur. Mol. Biol. Organ.) J.* 15:2893-2899.
- Hein, W.R., and A. Tunnacliffe. 1990. Characterization of the CD3  $\gamma$  and  $\delta$  invariant subunits of the sheep T cell antigen receptor. *Eur. J. Immunol.* 20:1505-1511.
- Hou, X., J. Dietrich, N. Odum, and C. Geisler. 1996. The cytoplasmic tail of Fc $\gamma$ RIIIA $\alpha$  is involved in signaling by the low affinity receptor for IgG. *J. Biol. Chem.* 271:22815-22822.
- Huang, L., and I.N. Crispe. 1993. Superantigen-driven peripheral deletion of T cells. Apoptosis occurs in cells that have lost the alpha/beta T cell receptor. *J. Immunol.* 151:1844-1851.
- Johnson, K.F., and S. Kornfeld. 1992. The cytoplasmic tail of the mannose 6-phosphate/insulin-like growth factor-II receptor has two signals for lysosomal enzyme sorting in the Golgi. *J. Cell. Biol.* 119:249-257.
- Krissansen, G.W., M.J. Owen, W. Verbi, and M.J. Crumpton. 1986. Primary structure of the T3  $\gamma$  subunit of the T3/T cell antigen receptor complex deduced from cDNA sequences: evolution of the T3  $\gamma$  and  $\delta$  subunits. *EMBO (Eur. Mol. Biol. Organ.) J.* 5:1799-1808.
- Krissansen, G.W., M.J. Owen, P.J. Fink, and M.J. Crumpton. 1987. Molecular cloning of the cDNA encoding the T3 $\gamma$  subunit of the mouse T3/T cell antigen receptor complex. *J. Immunol.* 138:3513-3518.
- Kruisbeek, A.M., and D. Amsen. 1996. Mechanisms underlying T-cell tolerance. *Curr. Opin. Immunol.* 8:233-244.
- Letourneur, F., and R.D. Klausner. 1992. A novel di-leucine motif and a tyrosine-based motif independently mediate lysosomal targeting and endocytosis of CD3 chains. *Cell*. 69:1143-1157.
- Levins, B., and C.A.L.S. Colaco. 1992. The CD3  $\gamma$ -chain, transmembrane signaling or recognition? *Immunogenetics*. 35:140-143.
- Littman, D.R., and S.N. Gettner. 1987. Unusual intron in the immunoglobulin domain of the newly isolated murine CD4 (L3T4) gene. *Nature (Lond.)*. 325:453-455.
- Lohse, M.J. 1993. Molecular mechanisms of membrane receptor desensitization. *Biochim. Biophys. Acta*. 1179:171-188.
- Marks, M.S., H. Ohno, T. Kirchhausen, and J.S. Bonifacino. 1997. Protein sorting by tyrosine-based signals: adapting to the Ys and wherefores. *Trends Cell Biol.* 7:124-128.
- Masui, H., A. Wells, C.S. Lazar, M.G. Rosenfeld, and G.N. Gill. 1991. Enhanced tumorigenesis of NR6 cells which express non-down-regulating epidermal growth factor receptors. *Cancer Res.* 51:6170-6175.
- Motta, A., B. Bremnes, M.A. Morelli, R.W. Frank, G. Saviano, and O. Bakke. 1995. Structure-activity relationship of the leucine-based sorting motifs in the cytosolic tail of the major histocompatibility complex-associated invariant chain. *J. Biol. Chem.* 270:27165-27171.
- Nesterov, A., R.C. Kurten, and G.N. Gill. 1995. Association of epidermal growth factor receptors with coated pit adaptins via a tyrosine phosphorylation-regulated mechanism. *J. Biol. Chem.* 270:6320-6327.
- Ohno, H., J. Stewart, M.C. Fournier, H. Bosshart, I. Rhee, S. Miyatake, T. Saito, A. Gallusser, T. Kirchhausen, and J.S. Bonifacino. 1995. Interaction of tyrosine-based sorting signals with clathrin-associated proteins. *Science (Wash. DC)*. 269:1872-1875.
- Pearse, B.M.F. 1988. Receptors compete for adaptors found in plasma membrane coated pits. *EMBO (Eur. Mol. Biol. Organ.) J.* 7:3331-3336.
- Pearse, B.M., and M.S. Robinson. 1990. Clathrin, adaptors, and sorting. *Annu. Rev. Cell Biol.* 6:151-171.
- Pieters, J., O. Bakke, and B. Dobberstein. 1993. The MHC class II-associated invariant chain contains two endosomal targeting signals within its cytoplasmic tail. *J. Cell Sci.* 106:831-846.
- Pond, L., L.A. Kuhn, L. Teyton, M. Schutze, J.A. Tainer, M.R. Jackson, and P.A. Peterson. 1995. A role for acidic residues in di-leucine motif-based targeting to the endocytic pathway. *J. Biol. Chem.* 270:19989-19997.
- Robinson, M.S. 1993. Adaptins. *Trends Cell Biol.* 2:293-297.
- Rocha, B., and H. von Boehmer. 1991. Peripheral selection of the T cell

- repertoire. *Science (Wash. DC)*. 251:1225–1228.
38. Sandoval, I.V., and O. Bakke. 1994. Targeting of membrane proteins to endosomes and lysosomes. *Trend Cell Biol.* 4:292–297.
  39. Sandoval, I.V., J.J. Arredondo, J. Alcalde, A.G. Noriega, J. Vandekerchove, M.A. Jimenez, and M. Rico. 1994. The residue leu(ile)475-ile(leu, val, ala)476, contained in the extended carboxyl cytoplasmic tail, are critical for targeting of the resident lysosomal membrane protein LIMP II to lysosomes. *J. Biol. Chem.* 269:6622–6631.
  40. Schonrich, G., U. Kalinke, F. Momburg, M. Malissen, A.M. Schmitt Verhulst, B. Malissen, G.J. Hammerling, and B. Arnold. 1991. Down-regulation of T cell receptors on self-reactive T cells as a novel mechanism for extrathymic tolerance induction. *Cell.* 65:293–304.
  41. Sheikh, H., and C.M. Isacke. 1996. A di-hydrophobic Leu-Val motif regulates the basolateral localization of CD44 in polarized Madin-Darby canine kidney epithelial cells. *J. Biol. Chem.* 271:12185–12190.
  42. Shin, J., C. Doyle, Z. Yang, D. Kappes, and J.L. Strominger. 1990. Structural features of the cytoplasmic region of CD4 required for internalization. *EMBO (Eur. Mol. Biol. Organ.) J.* 9:425–434.
  43. Shin, J., R.L. Dunbrack, S. Lee, and J.L. Strominger. 1991. Phosphorylation-dependent down-modulation of CD4 requires a specific structure within the cytoplasmic domain of CD4. *J. Biol. Chem.* 266:10658–10665.
  44. Sorokin, A., and G. Carpenter. 1993. Interaction of activated EGF receptors with coated pit adaptins. *Science (Wash. DC)*. 261:612–615.
  45. Sosa, M.A., B. Schmidt, K. von Figura, and A. Hille-Rehfeld. 1993. In vitro binding of plasma membrane-coated vesicle adaptors to the cytoplasmic domain of lysosomal acid phosphatase. *J. Biol. Chem.* 268:12537–12543.
  46. Sussman, J.J., J.S. Bonifacino, J. Lippincott-Schwartz, A.M. Weissman, T. Saito, R.D. Klausner, and J.D. Ashwell. 1988. Failure to synthesize the T cell CD3- $\zeta$  chain: structure and function of a partial T cell receptor complex. *Cell.* 52:85–95.
  47. Tafuri, A., J. Alferink, P. Moller, G.J. Hammerling, and B. Arnold. 1995. T cell awareness of paternal alloantigens during pregnancy. *Science (Wash. DC)*. 270:630–633.
  48. Trowbridge, I.S., J.F. Collawn, and C.R. Hopkins. 1993. Signal-dependent membrane protein trafficking in the endocytic pathway. *Annu. Rev. Cell Biol.* 9:129–161.
  49. Valitutti, S., S. Muller, M. Cella, E. Padovan, and A. Lanzavecchia. 1995. Serial triggering of many T-cell receptors by a few peptide-MHC complexes. *Nature (Lond.)*. 375:148–151.
  50. Valitutti, S., S. Muller, M. Dessing, and A. Lanzavecchia. 1996. Different responses are elicited in cytotoxic T lymphocytes by different levels of T cell receptor occupancy. *J. Exp. Med.* 183:1917–1921.
  51. Van den Elsen, P., B. Shepley, J. Borst, J.E. Coligan, A.F. Markham, S. Orkin, and C. Terhorst. 1984. Isolation of cDNA clones encoding the 20K T3 glycoprotein of human T-cell receptor complex. *Nature (Lond.)*. 312:413–418.
  52. Van den Elsen, P., B. Shepley, M. Cho, and C. Terhorst. 1985. Isolation and characterization of a cDNA clone encoding the murine homologue of the human 20K T3/T-cell receptor glycoprotein. *Nature (Lond.)*. 314:542–544.
  53. Vaux, D. 1992. The structure of an endocytosis signal. *Trends Cell Biol.* 2:189–192.
  54. Wegener, A.K., X. Hou, J. Dietrich, and C. Geisler. 1995. Distinct domains of the CD3- $\gamma$  chain are involved in surface expression and function of the T cell antigen receptor. *J. Biol. Chem.* 270:4675–4680.
  55. Wells, A., J.B. Welsh, C.S. Lazar, H.S. Wiley, G.N. Gill, and M.G. Rosenfeld. 1990. Ligand-induced transformation by a noninternalizing epidermal growth factor receptor. *Science (Wash. DC)*. 247:962–964.